Journal of the Serbian Chemical Society
JSCS-info@shd.org.rs • www.shd.org.rs/JSCS
J. Serb. Chem. Soc. *85* (4) 481–492 (2020)
JSCS–5316
UDC 547.853:620.193+519.677:544.6.004.12
Original scientific paper

Synthesis, characterization and theoretical studies of novel pyrimidine derivatives as potential corrosion inhibitors

ESVET AKBAS*, ELA YILDIZ and AHMET ERDOGAN

Department of Chemistry, Van Yuzuncu Yil University, 65080, Van, Turkey

(Received 26 March, revised 11 June, accepted 22 July 2019)

Abstract: In this study, five new pyrimidine derivatives were synthesized and characterized by characterization methods such as ^{1}H-NMR, ^{13}C-NMR, FT--IR and elemental analysis. The corrosion inhibition activity of the synthesized compounds was examined by theoretical calculation using DFT method at the level of B3LYP/6-31G (d,p). According to the calculations, 4-(6-benzoyl-2--benzylidene-3-oxo-7-phenyl-2,3-dihydro-5*H*-thiazolo[3,2-*a*]pyrimidin-5-yl)-benzoic acid (**6**) appears to be a good inhibitor for corrosion.

Keywords: corrosion inhibition; DFT; pyrimidine; characterization.

INTRODUCTION

Pyrimidines and their derivatives are organic compounds of special importance because of their wide spectrum of use in medicine, agrochemicals and in many biological processes. Several pyrimidine derivatives exhibit a diverse array of biological and pharmacological activities including anticonvulsant, antibacterial, antifungal, antiviral and anticancer properties.[1] This broad spectrum of biochemical targets has been enabled by the synthetic versatility of pyrimidine, which has allowed derivatisation of the ring nitrogens and C2/C4/C5/C6 carbon positions.[2] Pyrimidine derivatives are the components of many well established marketed drugs such as uramustine, piritrexim, tegafur, floxuridine, fluorouracil, cytarabine, methotrexate, etc. Moreover, the pyrimidine derivatives (mainly uracil, thiamine and cytosine) are essential parts in many natural products such as nucleic bases, vitamins, enzymes and hormones.[2]

The wide variety of biological activities observed for these compounds turned pyrimidine derivatives to be environmentally benign compounds. The requirement for a good corrosion inhibitor, *i.e.*, organic compounds which can donate electrons to an unoccupied d-orbital of a metal surface to form coordinate covalent bonds and can also accept free electrons from the metal surface using

* Corresponding author. E-mail: esvakbas@hotmail.com
https://doi.org/10.2298/JSC190326081A

Available on line at www.shd.org.rs/JSCS/
(CC) 2020 SCS.

their anti-bonding orbital to form feedback bonds, is also fulfilled by pyrimidine molecule. Hence pyrimidine derivatives are expected to be excellent corrosion inhibitors at industrial level, not only due to their efficiency but also due to their non-toxic nature.[1]

Acidic environments are widely used in several industrial operations, such as oil well acidification, acid pickling, acid cleaning and acid descaling, which generally lead to serious metallic corrosion. Despite the relatively limited corrosion resistance of carbon steel, it is widely used in marine applications, chemical processing, petroleum production and refining, construction and metal-processing equipment due to its excellent mechanical properties and low cost. Out of several methods, the use of corrosion inhibitor is one of the most important techniques for controlling the corrosion. Many organic inhibitors have been tried for the corrosion inhibition of steel, out of which organic compounds with more than one heteroatom containing π-electrons are found to exhibit high inhibiting properties by providing electrons which interact with metal surface.[3] However, the use of several heterocyclic inhibitors has caused negative effects on the environment because of their toxicity and nonbiodegradability. In this context, pyrimidine derivatives are found to attract great interest due to their environmentally benign properties.[4]

The quantum chemical calculations (QCCs) have been widely used in the reactivity of organic compounds for corrosion inhibition.[5] In this work, the theoretical calculations for the inhibition potentials were explained using QCCs based on density functional theory (DFT). The E_{HOMO} and E_{LUMO} energies of the molecules were calculated in the Gaussian09.[6]

The effectiveness of an inhibitor can be related not only to its spatial molecular structure, but also to their molecular electronic structure. According to frontier orbital theory, the reaction of reactants mainly occurred on highest occupied molecular orbital (HOMO) and lowest unoccupied molecular orbital (LUMO), and the formation of a transition state is due to an interaction between the frontier orbitals of the reactants. So, it was important to investigate the distribution of HOMO and LUMO for the exploration of inhibition mechanism. Organic substances with a higher energy level of HOMO easily donate electrons from HOMO to an empty orbital of appropriate acceptors and E_{LUMO} denotes the ability of a molecule to accept electrons.

The difference between E_{LUMO} and E_{HOMO} energies is called energy gap (ΔE). It was generally acknowledged that low values of ΔE will provide good inhibition efficiency, because the energy for removing an electron from the last occupied orbital will be low.[7]

For the theoretical calculation of the inhibitory effect of a molecule, it is necessary to know the ionization potential (I), the electron affinity (A), the chemical hardness-softness (S), the global electrophilicity index (ω), the interaction

(CC) 2020 SCS.

between the transmitted electron fraction index (ΔN) and the interaction between backdonations. All these values were calculated according to Shojaie *et al.*[8]

EXPERIMENTAL

Chemicals and instruments

All chemicals and solvents used in the experiments were supplied from the Turkish representative of Sigma Aldrich (St. Louis, MO) and Fluka (Buchs, Switzerland). All reactions were monitored by the thin layer chromatography (TLC). TLC plates were based on silica gel 60 F_{254} aluminum plates with a 0.2 mm layer thickness (Merck Co., Darmstadt, Germany). The spots in TLC were determined by UV lamp. Stuart (UK) SMP30 melting point apparatus was used to measure the melting points of the synthesized compounds. FT-IR spectra of the examined compounds were measured in the range of 4000–400 cm^{-1} using a Perkin Elmer Spectrum 100 FT-IR.

^{1}H- and ^{13}C-nuclear magnetic resonance (NMR) spectra of compounds were measured in DMSO-d_6 by using a Bruker (Billerica, MA) AVANCE DPX 400 MHz spectrometer at 400 and 100 MHz, respectively. Tetramethylsilane (TMS) was used as the internal reference. Elemental analyses were done using a Thermo Scientific (Pittsburgh, PA) Flash 2000 elemental analyzer. Full geometry optimizations of all the molecules were performed using Gaussian09. The physical, analytical and spectral data for the compounds are given in the Supplementary material to this paper.

Synthesis

*Ethyl 2-[(5-benzoyl-4-(3-nitrophenyl)-6-phenyl-3,4-dihydropyrimidin-2(1*H*)-ylidene)]acetate (**3**).* A solution of (4-(3-nitrophenyl)-6-phenyl-2-thioxo-1,2,3,4-tetrahydropyrimidin-5-yl)-phenylmethanone[9] (**1**, 1 mmol) and ethyl 2-bromoacetate (1 mmol) was refluxed for 6 h in dioxane (10 mL) in the presence of catalytic amount of pyridine (1 mL). Then the solvent was removed by a rotary evaporator. The resulting oily substance was treated with 1:1 ratio of HCl:H_2O (10 mL) and recrystallized from methanol.

*Ethyl 2-(5-benzoyl-4,6-diphenyl-3,4-dihydropyrimidin-2(1*H*)-ylidene)acetate (**4**).* The (4,6-diphenyl-2-thioxo-1,2,3,4-tetrahydropyrimidin-5-yl)phenylmethanone[10] (**2**, 1 mmol), ethyl 2-bromoacetate (1 mmol) and pyridine (1 mL) was refluxed in dioxane (10 mL) with for 6 h. Then the solvent was removed by a rotary evaporator. The resulting oily substance was treated with 1:1 ratio of HCl: H_2O (10 mL) and recrystallized from ethanol.

*4-(6-Benzoyl-2-benzylidene-3-oxo-7-phenyl-2,3-dihydro-5*H*-thiazolo[3,2-*a*]pyrimidin-5-yl)benzoic acid (**6**).* A mixture of **5**[11] (1 mmol), benzaldehyde (1 mmol) and anhydrous sodium acetate (1 mmol) in glacial acetic acid (10 ml) was heated under reflux for 4 h. The reaction mixture was kept overnight and the solid, thus separated, was filtered, washed with water and recrystallized from ethanol.

4-(6-benzoyl-3-oxo-7-phenyl-3,5-dihydro-2H-thiazolo[3,2-a]pyrimidin-5-yl)-N-*[(phenylamino)carbonyl]benzamine (**8**).* The 4-(6-benzoyl-3-oxo-7-phenyl-2,3-dihydro-5*H*-thiazolo-[3,2-*a*]pyrimidin-5-yl)benzoyl chloride (**7**) was obtained by the reaction of **5** with thionyl-chloride. The compound **5**[11] (1 mmol) and thionyl chloride (1 mL, 13.8 mmol) were refluxed on a steam bath for 6 h. The solvent was evaporated, and then the residue was dissolved in 10 mL of xylene. Thereafter, *N*-phenylurea and solution of compound **7** were boiled for 4 h. Then, the crude precipitate was filtered off and recrystallized from dioxane to give compound **8**.

*4-(7-Benzoyl-4-oxo-8-phenyl-3,4-dihydro-2*H*,6*H*-pyrimido[2,1-*b*][1,3]thiazin-6-yl)*-N,N-*diethylbenzamide (**11**).* The 4-(7-Benzoyl-4-oxo-8-phenyl-3,4-dihydro-2*H*,6*H*-pyrimido-

(CC) 2020 SCS.

[2,1-*b*][1,3]thiazin-6-yl)benzoic acid[11] (**9**, 1 mmol) and thionylchloride (1 mL, 13.8 mmol) were refluxed on a steam bath for 6 h. The solvent was evaporated, and then the residue was dissolved in 10 mL of xylene. Thereafter, diethylamine (5 mmol) and solution of compound **10** were boiled for 4 h. Then, the crude precipitate was filtered off and recrystallized from toluene to give of compound **11**.

RESULTS AND DISCUSSION

Synthesis

In this work, the obtained compounds were: ethyl 2-[5-benzoyl-4-(3-nitrophenyl)-6-phenyl-3,4-dihydropyrimidin-2(1*H*)-ylidene]acetate (**3**), ethyl 2-(5-benzoyl-4,6-diphenyl-3,4-dihydropyrimidin-2(1*H*)-ylidene)acetate (**4**), 4-(6-benzoyl-2-benzylidene-3-oxo-7-phenyl-2,3-dihydro-5*H*-thiazolo[3,2-*a*]pyrimidin-5-yl)benzoic acid (**6**), 4-(6-benzoyl-3-oxo-7-phenyl-2,3-dihydro-5*H*-thiazolo[3,2-*a*]pyrimidin-5-yl)-*N*-[(phenylamino)carbonyl]benzamide (**8**) and 4-(7-benzoyl-4-oxo-8-phenyl-3,4-dihydro-2*H*,6*H*-pyrimido[2,1-*b*][1,3]thiazin-6-yl)-*N*,*N*-diethylbenzamide (**11**).

The synthesis methodology of compounds **3** and **4** are similar to the Eschenmoser sulfide contraction. This reaction yields *β*-enaminocarbonyl derivatives of type IV by the elimination of sulphur from an episulfide intermediate (Scheme 1). This reaction was defined by Knott in 1955 and it was used for the synthesis of 1,3-dicarbonyl compounds from a thioester by Albert Eschenmoser.[12] This method requires a base and a tertiary phosphine. The method has a relevance to organic chemistry and has been notably applied in the vitamin B12 total synthesis.

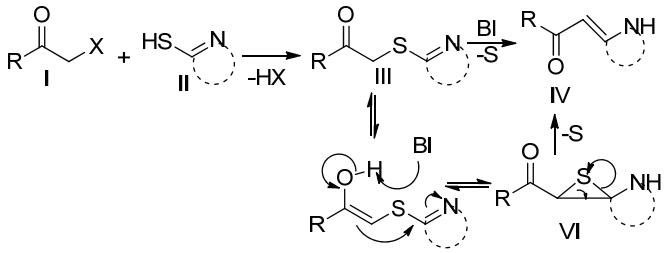

Scheme 1. The Eschenmoser coupling reaction.

This method generally requires tertiary phosphine, but instead of it we used pyridine as a catalyst and synthesized compounds **3** and **4** in a good yield (Scheme 2).

The IR spectra of **3** and **4** gave peaks at 3208–3061 cm^{-1} (NH) and 1622––1594 cm^{-1} (C=O) groups.

The ^{1}H-NMR spectra of the compound **3** showed *δ* 10.98 (*s*, 1H, NH), 10.12 (*s*, 1H, NH), 8.32–7.02 (*m*, 14H, $H_{arom.}$), 5.47 (*s*, 1H, C4H), 5.32 (*s*, 1H, =CH), 4.45 (*q*, 2H, OCH_2), 1.16 (*t*, 3H, CH_3) ppm and the ^{1}H-NMR spectra of the compound **4** showed *δ* 10.96 (*s*, 1H, NH), 10.11 (*s*, 1H, NH), 8.30–6.96 (*m*, 15H,

(CC) 2020 SCS.

$H_{arom.}$), 5.44 (*s*, 1H, C4H), 5.30 (*s*, 1H, =CH), 4.33 (*q*, 2H, OCH_2), 1.15 (*t*, 3H, CH_3) ppm.

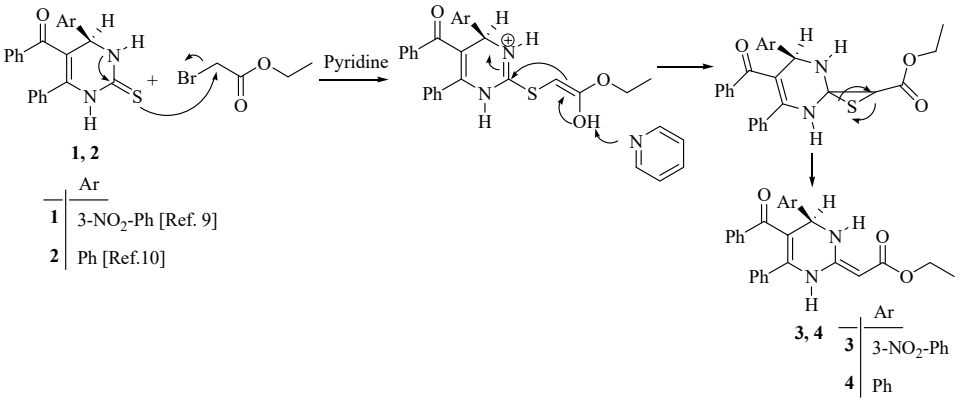

Scheme 2. Synthesis of the compounds **3** and **4**.

When acetic anhydride, *α*- and *β*-bromocarboxylic acids reacted with 4-(5--benzoyl-6-phenyl-2-thioxo-1,2,3,4-tetrahydropyrimidin-4-yl)benzoic acid the reactions resulted in 4-(6-benzoyl-3-oxo-7-phenyl-2,3-dihydro-5*H*-thiazolo[3,2--*a*]pyrimidin-5-yl)benzoic acid (**5**)[11] and 4-(7-benzoyl-4-oxo-8-phenyl-3,4--dihydro-2*H*,6*H*-pyrimido[2,1-*b*][1,3]thiazin-6-yl)benzoic acid (**9**)[11] derivatives, respectively. There are acidic protons at compound **5** (thiazole ring system), so the condensation reaction between thiazole (**5**) and benzaldehyde was performed and the compound **6** was obtained (Scheme 3).

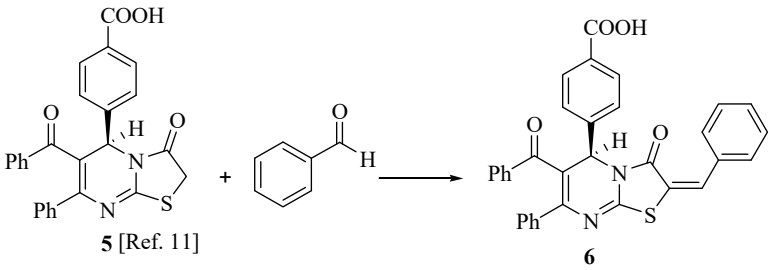

Scheme 3. Synthesis of the compound **6**.

On the other hand, after chlorination of compounds **5** and **9** with $SOCl_2$, the reaction of **5** with phenyl urea and the reaction of **9** with diethylamine resulted in compounds **8** and **11**, respectively (Scheme 4).

Calculation analysis

Full geometry optimizations of the all molecules were performed using DFT based on Beck's three parameter exchange functional and Lee–Yang–Parr[13] non-

(CC) 2020 SCS.

-local correlation functional (B3LYP) and the 6-31G(d,p) orbital basis sets in Gaussian09 program[6] (Fig. 1).

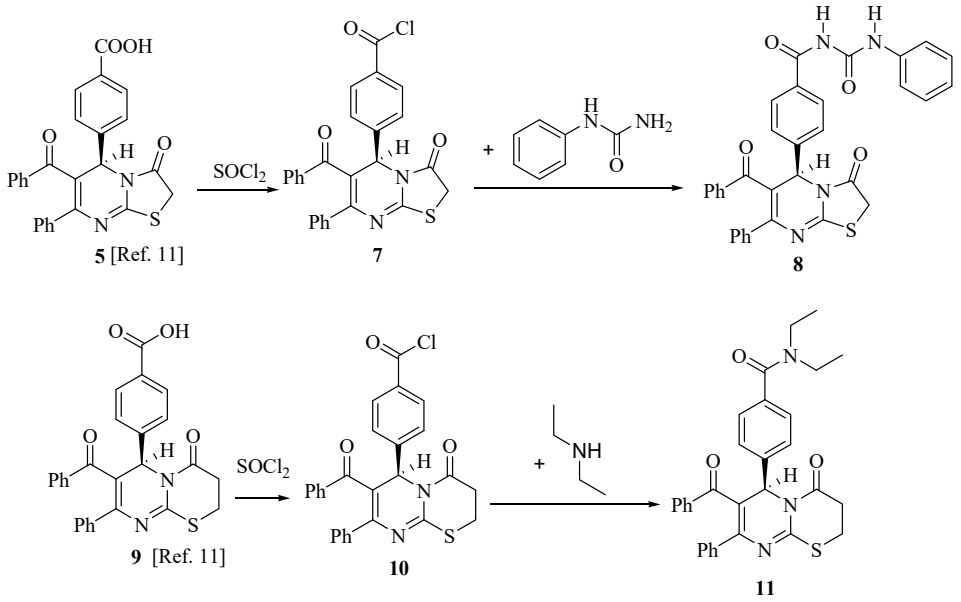

5 [Ref. 11] **7** **8** **9** [Ref. 11] **10** **11**

Scheme 4. Synthesis of the compounds **8** and **11**.

Very useful information can be obtained by the quantum chemical calculations to examine the corrosion inhibiting effects of organic compounds. The quantum chemical parameters all compounds such as μ, I, A, χ, η, w, S, ΔN and $\Delta E_{\text{backdonation}}$ were calculated according to Shojaie *et al.*[8] (Table I).

The inhibitory effect of a particular compound is usually attributed to adsorption of the molecule to the metal surface.[14] When the chemisorption occurs, one of the species entering the reaction behaves as an electron pair donor and the other acts as an electron pair acceptor.

The basic state geometry of the inhibitor and the structure of HOMO and LUMO play a role in the activity properties of the inhibitors. Remarkably, the shape of HOMO and LUMO is structurally dependent (Fig. 2). The electron density of the HOMO location in the inhibitors under study is mostly distributed on the atoms having a delocalized character showing that these atoms are the favorite adsorption sites

The inhibitors do not only donate electron to un-emissive d-orbitals of metals, but can also accept electrons from the d-orbital of the metal, which leads to a feedback bond. The electrons found in the HOMO can easily be donated. E_{HOMO} also play a most important role during corrosion inhibition course and this is directly related to the ionization potential. Increasing E_{HOMO} leads to higher inhibition effect.[15]

(CC) 2020 SCS.

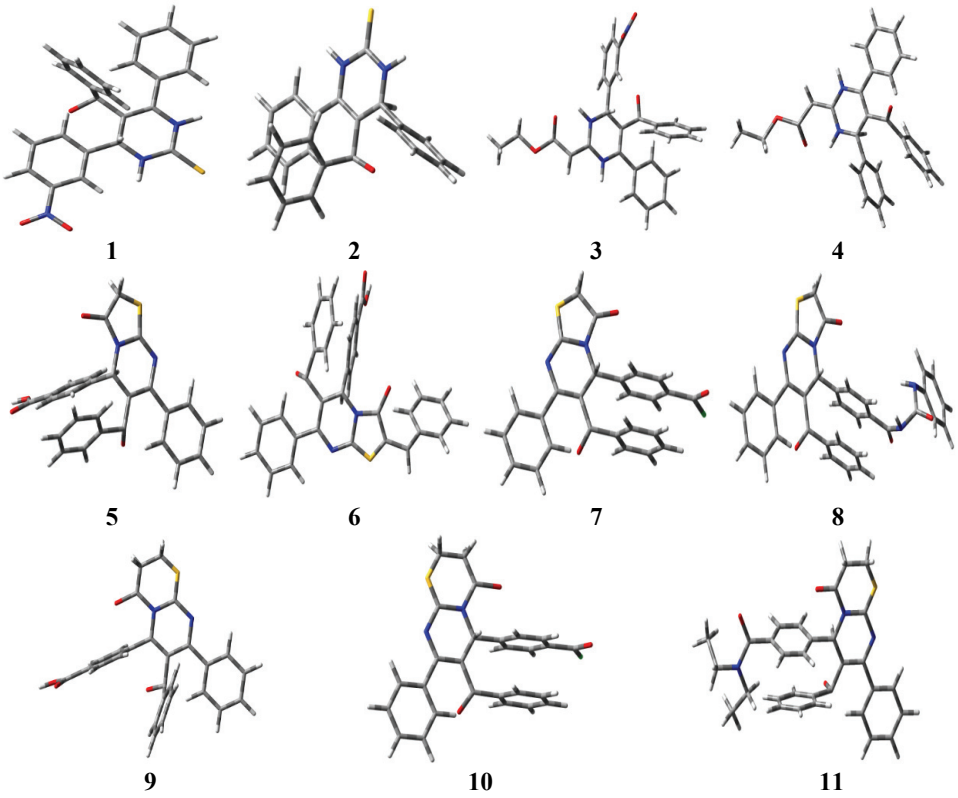

Fig. 1. Optimizations of all compounds.

TABLE I. The quantum chemical parameters for all compounds

Parameter	3	4	6	8	11
E_{HOMO} / eV	–6.8348	–6.0204	–4.2140	–5.7635	–4.7811
E_{LUMO} / eV	–3.2312	–2.0804	–4.0627	–2.5709	–1.7451
ΔE / eV	3.6036	3.9400	0.1513	3.1925	3.0359
Ionization potential, eV	6.8348	6.0204	4.2140	5.7635	4.7811
Electron affinity, eV	3.2312	2.0804	4.0627	2.5709	1.7451
Chemical hardness, eV	3.6036	3.9400	0.1513	3.1926	3.0360
Chemical softness, S / eV^{-1}	0.2775	0.2538	6.6093	0.3132	0.3294
Electronegativity, eV	5.0330	4.0504	6.2453	4.1672	3.2631
Transferred electrons fraction	0.2729	0.3743	0.0571	0.4437	0.6154
Dipole moment, D	9.0896	3.9613	2.6511	6.5956	3.8746
Electrophilicity index	11.4636	1.9913	0.5317	6.8129	2.4724
$\Delta E_{backdonation}$, eV^{-1}	–0.9009	–0.985	–0.0378	–0.7981	–0.7590

Another parameter of the molecular structure is the LUMO, which determines the polarizability of the compound. The lower the value of E_{LUMO}, the more probable that the molecule would accept electrons and the energy of the LUMO, which is directly related to the electron affinity.[16]

(CC) 2020 SCS.

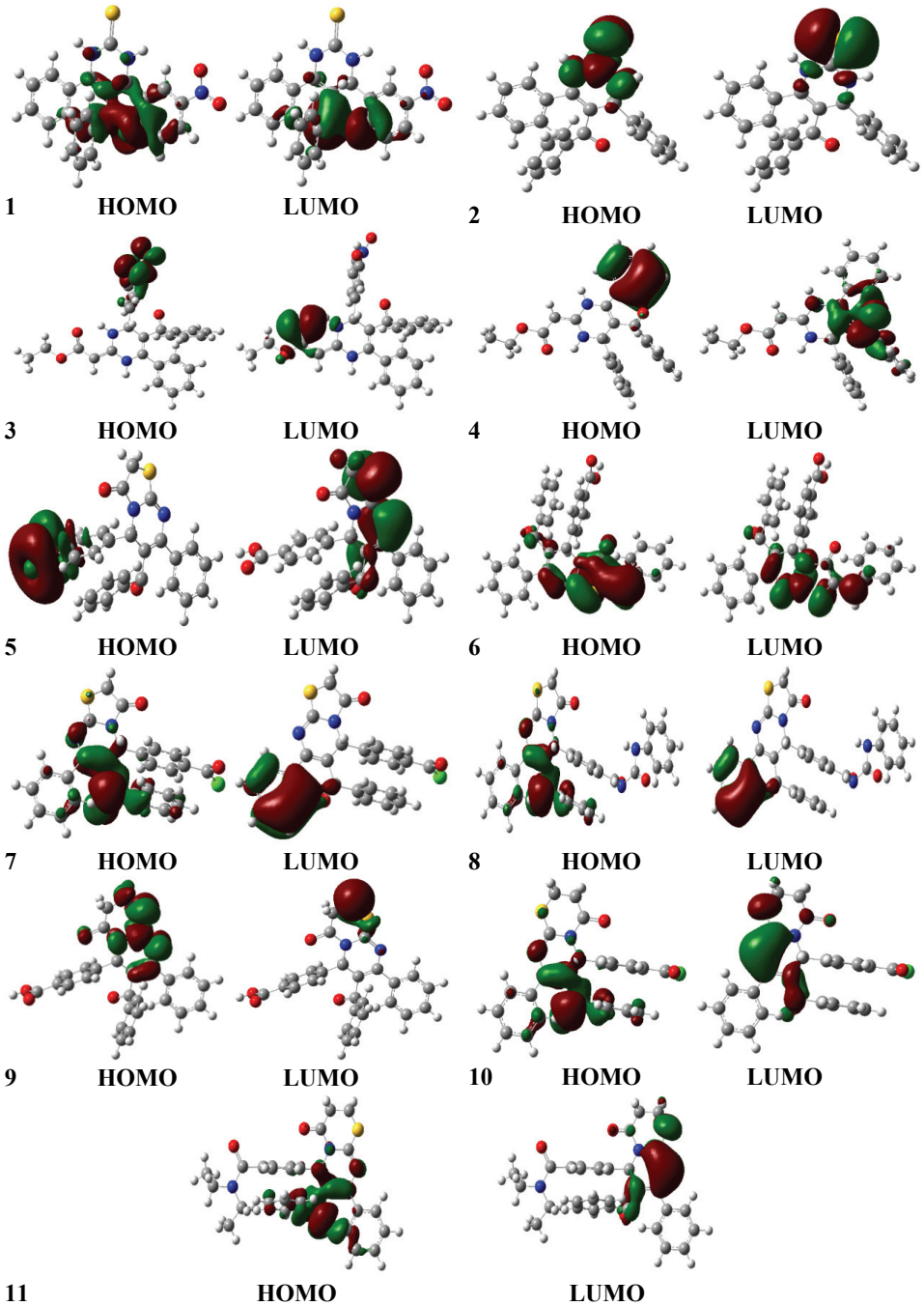

Fig. 2. Schematic representation of HOMO and LUMO molecular orbital of studied molecules.

(CC) 2020 SCS.

Similar relations were found between the rates of inhibition and energy gap. Larger values of the energy gap will provide low reactivity of a molecule. Lower values of the energy gap render a good inhibition efficiency, because the energy required to remove an electron from the lowest occupied orbital will be low.[15,16]

Dipole moment (μ/D*) is another important electronic parameter for corrosion inhibitors. The high value of the dipole moment probably increases the adsorption between the chemical compound and the metal surface.[15,16]

On the other hand, absolute hardness (η), softness (S), global electrophilicity index (ω) electrons transferred (ΔN), and $\Delta E_{\text{backdonation}}$ values are important properties used to measure the stability and reactivity of a molecule (Table I).[15,16]

The chemical hardness fundamentally signifies the resistance towards the deformation or polarization of the electron cloud of the atoms, ions or molecules under small perturbation of chemical reaction. A hard molecule has a large energy gap and a soft molecule has a small energy gap.[15,16]

The global electrophilicity index was introduced by Parr[17] as a measure of the energy lowering due to maximal electron flow between donor and acceptor. This index measures the ability of chemical species to accept electrons. A good, reactive nucleophile is characterized by low value of ω; and opposite to that, a good electrophile is characterized by a high value of ω. This new reactivity index measures the stabilization of energy, when the system acquires an additional electronic charge ΔN from the environment. If $\Delta N < 3.6$, the inhibition efficiency increases by increasing electron-donating ability of these inhibitors to donate electrons to the metal surface. The highest fraction of electrons transferred is associated with the best inhibitor.

According to the simple charge transfer model for donation and back-donation of charges, an electronic back-donation process might be occurring governing the interaction between the inhibitor molecule and the metal surface. The concept establishes that if both processes occur, namely charge transfer to the molecule and back-donation from the molecule, the energy change is directly proportional to the hardness of the molecule.[18–21]

The $\Delta E_{\text{backdonation}}$ implies that when $\eta > 0$ and $\Delta E_{\text{backdonation}} < 0$ the charge transfer to a molecule, followed by a backdonation from the molecule, is energetically favoured. In this context, it is possible to compare the stabilization among inhibiting molecules, since there will be an interaction with the same metal, then, it is expected that it will decrease as the hardness increases.[18–21]

According to the calculations, the compound **6** appears to be a good inhibitor for corrosion.

Molecular electrostatic potentials (MEP)

The MEP was run at B3LYP/6-31G (d,p) for molecule **6**. The MEP provides information about reactive sites for electrophilic and nucleophilic attack as well

* 1 D = 3.33564×10^{-30} C m

(CC) 2020 SCS.

as hydrogen-bonding interactions in molecules. The MEP for molecule **6** given in Fig. 3 was studied. The electrostatic potentials at the surface are represented by different colours; red, blue and green represent the regions of negative, positive and zero electrostatic potential respectively. In addition, the negative regions (red colour) of MEP are related to electrophilic reactivity, and the positive regions (blue colour) are related to the nucleophilic reactivity.

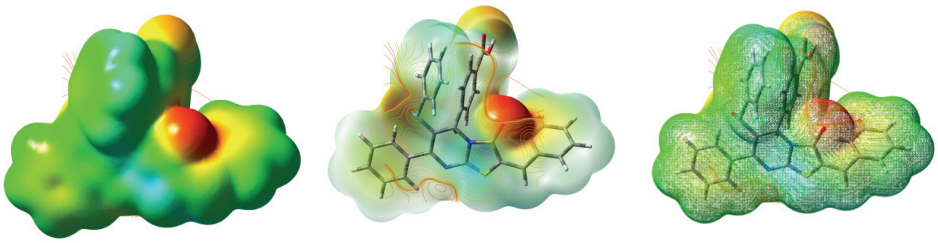

Fig. 3. The molecular electrostatic potentials maps for compound **6**.

CONCLUSION

The pyrimidine derivatives were synthesized and all structures determined using FT-IR, $^{1}H/^{13}C$-NMR and elemental analyses. The compounds were investigated as corrosion inhibitors using density functional theory (DFT) at the level of B3LYP/6-31G (d,p).

As presented in Table I, the compound which has the lowest energetic gap is the compound **6** (ΔE = –3.6416 eV). This lower gap allows it to be the softest molecule. The compound that has the highest HOMO energy is the compound **6** (E_{HOMO} = –0.4212 eV). This higher energy allows it to be the best electron donor.

The two properties like I (ionization potential) and A (affinity) are so important that the determination of these two properties allows us to calculate the absolute electronegativity (χ) and the absolute hardness (η). These two parameters are related to the one-electron orbital energies of the HOMO and LUMO, respectively. Compound **6** has the lowest value of the ionization potential (I = = 4.2140 eV), so it is the best electron donor. Compound **6** also has the largest value of the affinity (A = 4.0627 eV), so it is the best electron acceptor. The chemical reactivity varies with the structure of molecules

Compound **6** has the lowest value of the ionization potential (I = 4.2140 eV), so it is the best electron donor. Compound **6** also has the largest value of the affinity (A = 4.0627 eV), so it is the best electron acceptor. The chemical reactivity varies with the structure of molecules. The value of ω for compound **6** (ω = = –0.9650 eV) indicates that it is a stronger nucleophile than all other compounds.

According to all of the calculations, the compound **6** appears to be a better inhibitor for corrosion than other molecules.

(CC) 2020 SCS.

SUPPLEMENTARY MATERIAL

Additional data are available electronically from http://www.shd.org.rs/JSCS/, or from the corresponding author on request.

ИЗВОД

СИНТЕЗА, КАРАКТЕРИЗАЦИЈА И ТЕОРИЈСКА СТУДИЈА НОВИХ ДЕРИВАТА ПИРИМИДИНА КАО ПОТЕНЦИЈАЛНИХ АГЕНАСА ЗА СУЗБИЈАЊЕ КОРОЗИЈЕ

ESVET AKBAS, ELA YILDIZ и AHMET ERDOGAN

Department of Chemistry, Van Yuzuncu Yil University, 65080, Van, Turkey

У овој студији синтетизовано је и карактерисано пет деривата пиримидина методама карактеризације попут ^{1}H-NMR, ^{13}C-NMR, FT-IR и елементалне анализе. Антикорозивна активност синтетисаних једињења испитана је теоријским израчунавањима користећи DFT метод на B3LYP/6-31G(d,p) нивоу. Израчунавања показују да би 4-(2-бензилиден-6-бензоил-3-оксо-7-фенил-2,3-дихидро-5*H*-тиазоло[3,2-*a*]пиримидин-5-ил)-бензоева киселина (**6**) могла бити добар инхибитор корозије.

(Примљено 26. марта, ревидирано 11 јуна, прихваћено 22. јула 2019)

REFERENCES

1. K. Rasheeda, V. D. P. Alva, P. A. Krishnaprasad S. Samshuddin, *Int. J. Corros. Scale Inhib.* **7** (2018) 48 (http://dx.doi.org/10.17675/2305-6894-2018-7-1-5)
2. S. Samshuddin, B. Narayana, H. S. Yathirajan, T.Gerber, E. Hosten, R. Betz, *Acta Crystallogr., Sect. E: Struct. Rep. Online* **68** (2012) 3271 (https://doi.org/10.1107/S1600536812044662)
3. Yu. I. Kapustin, A. G. Kholodkova, T. A. Vagramyan, *Int. J. Corros. Scale Inhib.* **7** (2018) 1 (http://dx.doi.org/10.17675/2305-6894-2018-7-1-1)
4. E. Akbas, A. Ruzgar, E. Sahin, E. Ergan, *J. Heterocycl. Chem.* **56** (2019) 1003 (https://doi.org/10.1002/jhet.3483)
5. E. Akbas, E. Ergan, E. Sahin, S. Ekin, M. Cakir, Y. Karakus, *Phosphorus, Sulfur Silicon Relat. Elem.* **194** (2019) 796 (https://doi.org/10.1080/10426507.2018.1550489)
6. *Gaussian 09, Revision E.01*, Gaussian, Inc., Wallingford, CT, 2009 (http://gaussian.com/g09citation/)
7. G. Gece, *Mater. Corros.* **64** (2013) 940 (https://doi.org/10.1002/maco.201106482)
8. F. Shojaie, N. M. Baghini, *Int. J. Ind. Chem.* **6** (2015) 297 (https://doi.org/10.1007/s40090-015-0052-x)
9. E. Akbas, F. Aslanoglu, B. Anil, A. Sener, *J. Heterocycl. Chem.* **45** (2008) 1457 (https://doi.org/10.1002/jhet.5570450532)
10. E. Akbas, F. Aslanoglu, *Phosphorus Sulfur, Silicon Relat. Elem.* **183** (2008) 82 (https://doi.org/10.1080/10426500701557021)
11. E. Akbas, A. Erdogan, E. Ergan, M. Gulcan, A. Ruzgar, *J. Chem. Soc. Pak.* **39** (2017) 269 (https://doi.org/10.1007/s12039-019-1602-0)
12. A. Eschenmoser, C. E. Wintner, *Science* **196** (1977) 1410 https://doi.org/10.1126/science.867037)
13. C. Lee, W. Yang, R. G. Parr, *Phys. Rev. B: Codens. Matter Mater. Phys.* **37** (1988) 785 (https://doi.org/10.1103/PhysRevB.37.785)
14. S. A. X. Stango, U. Vijayalakshmi, *J. Asian Ceram. Soc.* **6** (2018) 20 (https://doi.org/10.1080/21870764.2018.1439608)
15. G. Gece, *Corros. Sci.* **50** (2008) 2981 (https://doi.org/10.1016/j.corsci.2008.08.043)

(CC) 2020 SCS.

16. A. Popova, M. Christov, A. Zwetanova, *Corros. Sci.* **49** (2007) 2131 (https://doi.org/10.1016/j.corsci.2006.10.021)
17. R. G. Parr, L. Szentpaly, *J. Am. Chem. Soc.* **121** (1999) 1922 (https://pubs.acs.org/doi/10.1021/ja983494x)
18. P. K. Chattaraj, U. Sarkar, D. R. Roy, *Chem. Rev.* **106** (2006) 2065 (https://doi.org/10.1021/cr040109f)
19. C. Farley, N. V. S. D. K. Bhupathiraju, B. K. John, C. M. Drain, *J. Phys. Chem. A* **120** (2016) 7451 (https://pubs.acs.org/doi/10.1021/acs.jpca.6b07024)
20. A. D. Becke, *J. Chem. Phys*. **96** (1992) 2155 (https://doi.org/10.1063/1.462066)
21. A. D. Becke, *J. Chem. Phys.* **98** (1993) 5648 (https://doi.org/10.1063/1.464913).

(CC) 2020 SCS.